JOC Article

Redox Electron-Transfer Reactions: Electrochemically Mediated Rearrangement, Mechanism, and a Total Synthesis of Daucene

Young Sam Park and R. Daniel Little*

Department of Chemistry & Biochemistry, University of California, Santa Barbara, California 93106

little@chem.ucsb.edu

Received June 3, 2008

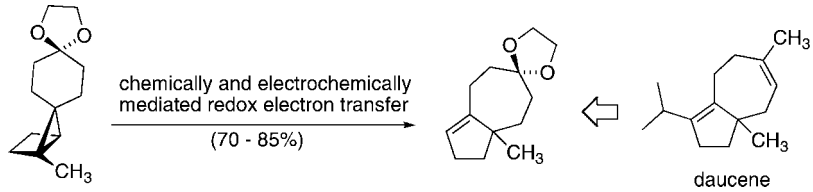

The term "housane" refers to molecules possessing a bicyclo[2.1.0]pentane core. One was designed, synthesized, and used as a precursor of daucene, a member of the carotane class of sesquiterpenes. The total synthesis was completed, thereby marking the first time that housane-derived cation radicals have been used as the key intermediate in the synthesis of a natural product. The transformation used in the construction and featured in the text involves an oxidation to generate the cation radical via either a chemically or an electrochemically mediated electron transfer, the latter process using tris(*p*-bromophenyl)amine as the mediator. The two methods are compared, and guiding principles are formulated to assist in deciding how best to implement each. Both processes afford an unfavorable equilibrium state that is subsequently drained toward the product by two irreversible events, viz., a 1,2 carbon migration to the site that best stabilizes a positive charge and a second electron transfer, this time being a highly exothermic reduction of the rearranged species to generate the neutral product. A mechanistic proposal calling for the use of a catalytic quantity of the electrochemical mediator and the consumption of exceptionally small quantities of current is advanced. Experimental deviations from these predictions are noted, and a rationale to account for them is presented. Finally, significant differences were noted between the cyclic voltammograms of housanes bearing a CH_2OR substituent rather than a methyl group at the bridgehead carbon. Those having the inductively withdrawing group displayed broad and ill-defined curves. The differences were investigated quantum mechanically, and a stereoelectronic argument is formulated stating that broadness of the curve for the $ROCH_2$-substituted systems is the result of a time-averaged sampling of the HOMO energies over the distribution of conformers. The possible generality of the stereoelectronic effect is noted.

Introduction

We recently described the electrochemically mediated rearrangement of the benzyloxymethyl-substituted housane **1** to the hydrindene adduct **3** via the cation radical intermediate **4**.[1] Tris(4-bromophenyl)amine (**2**) served as a redox mediator. When it was oxidized at a potential of +0.9 V (vs $Ag/AgNO_3$), the resulting aminium cation radical served as an oxidizing agent toward the housane, despite the fact that the direct anodic oxidation of the housane requires a potential of ca. 1.3−1.4 V. The thermodynamic impasse that drives the unfavorable electron transfer equilibrium is overcome by the subsequent transformations that lead, irreversibly, to the product **3**.

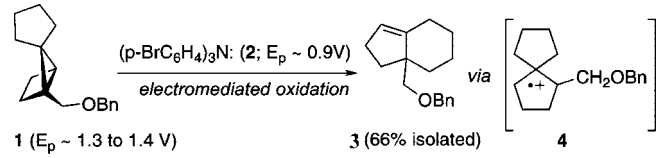

To date, our studies have focused upon gaining an understanding of the properties of the cation radicals that are generated via the oxidation of housanes, with an eye toward applying the knowledge gained in this manner toward the total synthesis of

(1) (a) Park, Y. S.; Wang, S. C.; Tantillo, D. J.; Little, R. D. *J. Org. Chem.* **2007**, *72*, 4351–4357. (b) Gerken, J. B.; Wang, S. C.; Preciado, A. B.; Park, Y. S.; Nishiguchi, G.; Tantillo, D. J.; Little, R. D. *J. Org. Chem.* **2005**, *70*, 4598–4608.

10.1021/jo801199s CCC: $40.75 © 2008 American Chemical Society
Published on Web 07/30/2008

natural products. Toward this end, we have synthesized housane **5**, a potential precursor to the sesquiterpene daucene (**6**).[2] Successful application of the chemistry requires that the rearrangement of the cation radical **8** proceed regiospecifically, or at least with a large preference for migration toward the site to which the methyl group is appended.

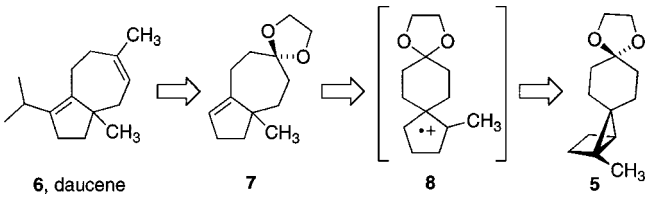

Herein, we report (a) the first occasion where the transformation has been applied to the construction of a seven membered ring, (b) the contrasting results obtained from the use of tris(4-bromophenyl)aminium antimonate (**9**) vs the electrochemically generated tris(4-bromophenyl)aminium cation radical (**10**) as the oxidant of housane **5**, (c) the role of added base in shutting down unwanted side reactions involving the antimonate chemistry, (d) completion of a total synthesis of daucene (**6**), (e) a discussion of stereoelectronic factors that govern the oxidizability of substituted housanes, and (f) an assessment of the mechanism for trisarylaminium cation radical induced oxidations.

Synthesis of Daucene Precursors Diazene 14 and Housane 5

Our efforts began with the known spirocyclic enone **11** (Scheme 1).[3] It was readily converted to the housane precursor

SCHEME 1. Synthesis of Diazene 14 and Its Conversion to Housane 5[a]

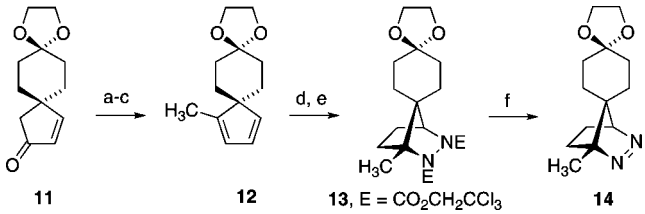

[a] Reagents: (a) LDA, THF, CH_3I (45%); (b) $NaBH_4$, $CeCl_3 \cdot 7H_2O$, MeOH (79%); (c) Ms_2O, Et_3N, PhH (89%); (d) $(Cl_3CCH_2O_2CN)_2$, CH_2Cl_2; (e) H_2, EtOAc (92%, two steps); (f) KOH, EtOH; $K_2Fe(CN)_6$, H_2O (80%).

14 via a sequence that began with the alkylation of the enolate derived from **11** and a subsequent Luche reduction followed by mesylation and elimination. Except for the poor yield encountered in the alkylation, the transformations proceeded smoothly and in good yield to deliver the functionalized spirocyclic cyclopentadiene **12**. A Diels−Alder reaction of the diene with bis(trichloroethoxy) azodicarboxylate and the ensuing reduction of the $\Delta^{5,6}\pi$ bond using catalytic hydrogenation provided the anticipated biscarbamate in high yield (92%). Hydrolysis followed by oxidation resulted in diazene **14** in an 80% yield. Irradiation of **14** using a simple UV handlamp (365 nm setting) produced the functionalized spirocyclic housane **5** in an 89% yield.

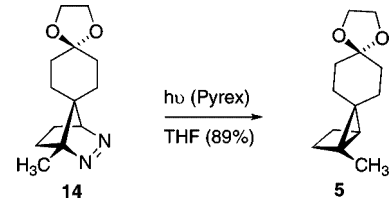

Results and Discussion

The Rearrangement. Chemical Vs Electrochemically Mediated Electron Transfer. Treatment of **5** with 40 mol % of tris(4-bromophenyl)aminium hexachloroantimonate **9** *in the presence of 2,6-di-tert-butylpyridine* as an acid scavenger afforded a single rearrangement product **7** in an 85% yield.[4] This transformation marks the first instance wherein the rearrangement of the cation radical from a housane has been used to construct a seven-membered ring to access the bicyclo[5.3.0] framework, one that is common to a large number of natural products.[5] In the absence of 2,6-di-*tert*-butylpyridine, the chemistry takes an entirely different course, leading to the formation of the spirocyclic alkene **15**, the product of a Lewis acid promoted ($SbCl_5$; vide infra) ring opening of the strained framework.[6]

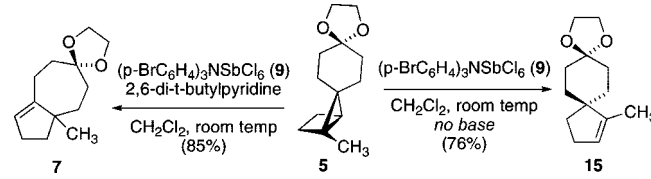

The desired adduct **7** was also conveniently obtained by using tris(4-bromophenyl)amine **2** as a redox mediator.[1] The reaction was carried out in a simple cylindrical glass vial fitted with a Pt anode and an reticulated glassy carbon (RVC) cathode, a 0.1 M solution of n-Bu_4NBF_4 in acetonitrile, and 20−40 mol % of tris(4-bromophenyl)amine **2**.[7] The oxidation was conducted

(2) As a component in flavors and fragrances, see: Mazzoni, V.; Tomi, F.; Casanova, J. *Flavour Fragr. J.* **1999**, *14*, 268–272. For previous synthetic efforts, see: (a) Pigulevskii, G. V.; Kivaleva, V. I. *Doklady Akad. Nauk S.S.S.R.* **1961**, *141*, 1382. (b) Sriraman, M. C.; Nagasampagi, B. A.; Pandey, R. C.; Dev, S. *Tetrahedron* **1973**, *29*, 985–991. (c) Audenaert, F.; Keukeleire, D. D.; Vandewalle, M. *Tetrahedron* **1987**, *43*, 5593–5604. (d) Naegeli, P.; Kaiser, R. *Tetrahedron Lett.* **1972**, *13*, 2013–2016. (e) Seto, H.; Fujimoto, Y.; Tatsuno, T.; Yoshioka, H. *Synth. Commun.* **1985**, *15*, 1217–1224. (f) Mehta, G.; Krishnamurthy, N. *Synth. Commun.* **1985**, *18*, 1267–1274. (g) Yamasaki, M. *J. Chem. Soc., Chem. Commun.* **1972**, 606–607. (h) deBroissia, H.; Levisalles, J.; Rudler, H. *Bull. Soc. Chim. Fr.* **1972**, 4314–4318.

(3) Srikrishna, A.; Kumar, P. P. *Tetrahedron* **2000**, *56*, 8189–8195.

(4) That the rearrangement occurred toward the proximal methyl group was confirmed by the appearance of a vinyl proton signal at 5.32 ppm that is consistent with a proximal migration to the tertiary bridgehead carbon. A methyl group signal appeared at 0.95 ppm, far upfield of that expected for the allylic methyl group that would have been present had the migration occurred in the opposite direction. Resonances appearing at 124.1 and 152.7 ppm of the ^{13}C NMR spectrum confirmed the presence of the alkene.

(5) Fraga, B. M. *Nat. Prod. Rep.* **1992**, *9*, 217–241.

(6) (a) Ciminale, F.; Lopez, L.; Farinola, G. M.; Sportelli, S.; Nacci, A. *Eur. J. Org. Chem.* **2002**, 3850–3854. (b) Ciminale, F.; Lopez, L.; Farinola, G. M.; Sportelli, S. *Tetrahedron Lett.* **2001**, *42*, 5685–5687. These researchers showed that the antimonate salt releases $SbCl_5$ via an equilibrium process. The base, therefore, suppresses Lewis acid promoted pathways. That antimonate that is not consumed by complexation is available to serve as the oxidizing agent that is required to initiate the rearrangement. Given the irreversibility of the complexation, it is not surprising that one must increase the amount of the antimonate salt in order to assure that the desired reaction proceeds to completion. In practice, after 10 min in the presence of 20 mol % of the antimonate salt, the blue-green color corresponding to the presence of $(BrC_6H_4)_3N^{\bullet+}$ changed to a dark yellow. An additional 20 mol % of the antimonate was needed to maintain the blue color and drive the reaction to completion.

(7) A larger than customary amount of the trisarylamine was used in an effort to force the reaction to completion with the expectation of an increase in the yield. Unfortunately, this did not prove to be the case. Rather than having the desired outcome, the presence of additional mediator led to the oxidation of the product, with the formation of an unidentified byproduct as soon as the starting material was consumed.

at the potential of the amine rather than the housane (~+0.9 V). The electrolysis proceeded smoothly and resulted in a 70% yield of the [5.3.0] adduct **7**. In contrast with the chemical electron transfer protocol, the electrochemical process did not require the addition of a base; if needed, the tris(4-bromophenyl)amine itself can behave in that manner. Nevertheless, we advocate the use of an acid scavenger in both the chemical electron transfer and electrochemical oxidations.

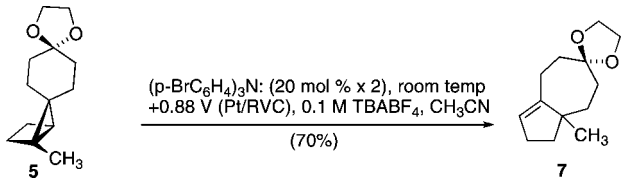

Completion of the Total Synthesis. The product of the rearrangement step, **7**, was converted to daucene **6**, in the straightforward manner illustrated in Scheme 2, thereby demonstrating that housane-derived cation radicals *can* serve as useful intermediates in natural product synthesis. The spectral data for synthetic daucene matched those reported in the literature.[8]

SCHEME 2. Completion of the Daucene Synthesis[a]

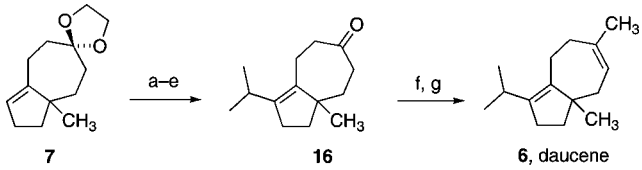

[a] Reagents: BH_3, THF; NaOH, H_2O_2; (b) PDC, CH_2Cl_2, molecular sieves (56%, steps a + b); (c) *i*-PrLi, $CeCl_3$ (anhyd), THF; (d) Ms_2O, Et_3N, PhH (45%, two steps); (e) 70% $HClO_4$, $CHCl_3$ (48% to equilibrate alkene isomers and remove the ketal); (f) MeMgBr, THF, $CeCl_3$ (anhyd); (g) Ms_2O, Et_3N, PhH (27%, two steps + 26% starting material).

Mechanism. We propose that the rearrangement of **5** to **7** occurs in the manner shown in Scheme 3. The sequence begins with oxidation of tris(*p*-bromophenyl)amine **2** at the anode. The resulting aminium cation radical **10**, in turn, serves as an oxidizing agent toward the housane, converting the latter to the ring-opened cation radical **8** and establishing an equilibrium between the components **5**, **8**, **2**, and **10**. Consistent with the existence of an equilibrium process is the observation that the starting material is consumed more rapidly when additional quantities of the amine are added. That the first step is a bottleneck is supported by the accumulation and gradual disappearance of a blue-green color corresponding to the amminium cation radical **10** at the anode while the comparatively slow electron transfer occurs.

SCHEME 3. Proposed Mechanism[a]

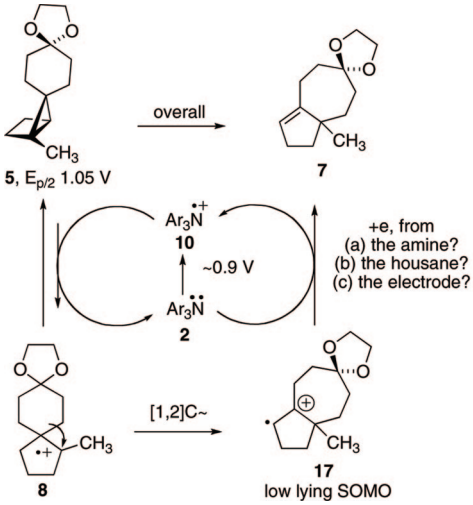

[a] Notice the blue-green color of the amminium cation radical near the anode.

The ability of the aminium cation radical **10** to affect the oxidation and return to the redox equilibrium as the neutral amine **2** is clearly evident by the catalytic current that is evident in the voltammogram illustrated in Figure 1.

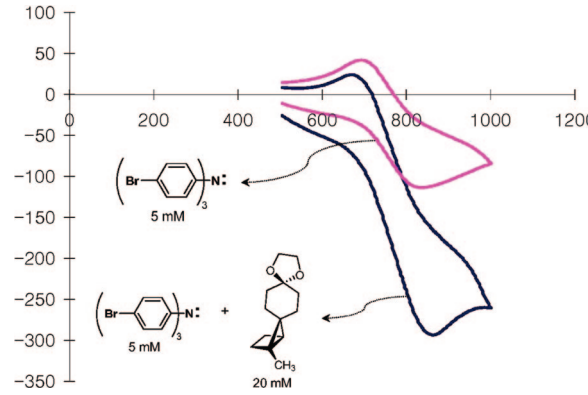

FIGURE 1. Appearance of a catalytic current in the electromediated redox process.

To overcome the thermodynamic impasse that accompanies the initial electron transfer event, there must be one or more irreversible follow-up reactions in order to shift the equilibrium to the product side. The conversion of the rearranged cation radical **17** to the product **7** clearly meets this requirement. Its SOMO energy must be very deep, indicating that it ought to be exceedingly easy to reduce.[9] While thermodynamically favorable, the rate of this process will be limited by the low concentration of **17**. There are two reasonable sources of the electron: (1) the amine **2** and (2) the starting housane **5**. Based upon experiment and calculations, the amine is easier to oxidize than the housane and is, therefore, the more likely reducing agent; the HOMO energy for the amine is calculated to be −5.49 eV, while that for the housane is nearly 1 eV deeper at −6.43 eV (B3LYP/6-31G(d) calculations).[9] Thus, while either reductant should easily be capable of transferring an electron to **17**, the amine is more likely since the HOMO−SOMO gap is smaller for this redox pair.

(8) We are well aware of the fact that the sequence from the rearrangement product **7** to daucene could have been conducted in a more elegant manner. We opted, instead, for an expeditious approach and to focus our attention upon gaining an understanding of the fundamental chemistry of cation radicals and mediated redox processes.

(9) Shao, Y.; Molnar, L. F.; Jung, Y.; Kussmann, J.; Ochsenfeld, C.; Brown, S. T.; Gilbert, A. T. B.; Slipchenko, L. V.; Levchenko, S. V.; O'Neill, D. P.; DiStasio, R. A., Jr.; Lochan, R. C.; Wang, T.; Beran, G. J. O.; Besley, N. A.; Herbert, J. M.; Lin, C. Y.; Van Voorhis, T.; Chien, S. H.; Sodt, A.; Steele, R. P.; Rassolov, V. A.; Maslen, P. E.; Korambath, P. P.; Adamson, R. D.; Austin, B.; Baker, J.; Byrd, E. F. C.; Dachsel, H.; Doerksen, R. J.; Dreuw, A.; Dunietz, B. D.; Dutoi, A. D.; Furlani, T. R.; Gwaltney, S. R.; Heyden, A.; Hirata, S.; Hsu, C.-P.; Kedziora, G.; Khalliulin, R. Z.; Klunzinger, P.; Lee, A. M.; Lee, M. S.; Liang, W. Z.; Lotan, I.; Nair, N.; Peters, B.; Proynov, E. I.; Pieniazek, P. A.; Rhee, Y. M.; Ritchie, J.; Rosta, E.; Sherrill, C. D.; Simmonett, A. C.; Subotnik, J. E.; Woodcock, H. L., III; Zhang, W.; Bell, A. T.; Chakraborty, A. K.; Chipman, D. M.; Keil, F. J.; Warshel, A.; Hehre, W. J.; Schaefer, H. F.; Kong, J.; Krylov, A. I.; Gill, P. M. W.; Head-Gordon, M. *Phys. Chem. Chem. Phys.* **2006**, *8*, 3172.

Once the initial oxidation of the amine occurs, the sequence ought to continue without consuming additional current until the starting material has disappeared, or at least until its concentration has been greatly diminished. Unfortunately, this prediction does not accord with experiment; more than 1 F/mol of charge was required to completely consume the starting material. Fry and co-workers noted a similar inefficiency in their recent publication describing the oxidative cleavage of electron deficient stilbenes using the aminium cation radical **10** as an oxidant.[10] Given the slowness of an initial electron-transfer step, they suggested that there was time enough for the aminium cation radical **10** to migrate to the cathode and be reduced to form the neutral amine, thereby interrupting the catalytic cycle and reducing its efficiency. We believe that this rationale also accounts for our observations. Future investigations will focus upon overcoming this limitation.

Redox Potentials. The cyclic voltammograms for housanes **1**, **5**, and **18b** are significantly different; note Figure 2.[11] Those for the benzyloxymethyl- and hydroxymethyl-substituted systems **1** and **18b** display broad, ill-defined curves that render it impossible to determine either E_p or $E_{p/2}$. In contrast, the voltammogram for **5** is well defined, giving rise to a clearly defined peak from which one can easily determine E_p. Notice also that the peak appears at a potential that is clearly less positive than either of the other two substrates, suggesting that **5** is easier to oxidize.

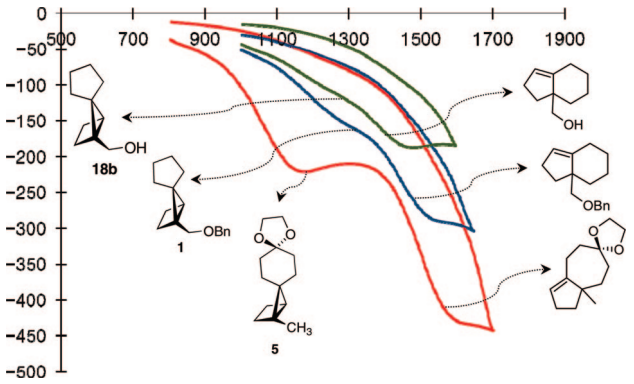

FIGURE 2. Cyclic voltammograms corresponding to three housanes. Glassy carbon anode, Pt wire cathode, $Ag/AgNO_3$ reference electrode, 0.1 M n-Bu_4NBF_4 supporting electrolyte in CH_3CN, 200 mV/s scan rate. Note that the housane concentration was 20 mM for **1** and **5** but 10 mM for **18b**. In each instance, the second "peak" was shown to correspond to the oxidation product by comparing the curves with authentic substances.

Why are the voltammograms for the systems bearing electronegative groups broad and ill-defined? And why is the peak for the methyl-substituted system shifted to a less positive value (i.e., easier to oxidize)? To address the latter, we explored the notion that the shift in the observed potential from one system to another might reflect differences in the rates of the reactions that drain the initially unfavorable electron-transfer equilibrium toward the product. This idea is illustrated in Scheme 4 for the conversion of cation radical **6** to **17** and **19** to **20**. Should the expansion leading to the seven-membered ring be faster than the expansion to the six, then the redox equilibrium ought to

SCHEME 4. Which Is Faster: Expansion to a Six- or a Seven-Membered Ring?

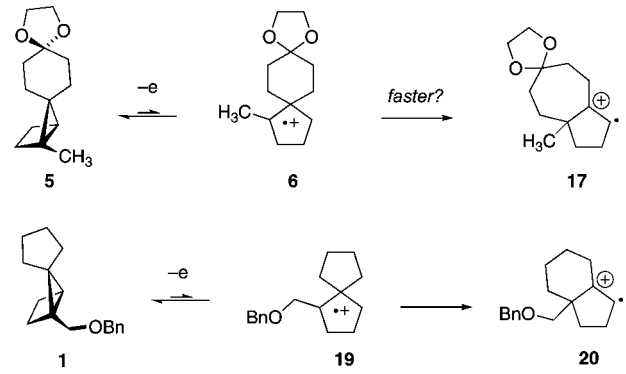

reflect the difference, viz., the faster the process, the less positive the oxidation peak.[12] In practice, AM1 calculations show that the activation energy for the rearrangement leading to the six-membered ring (17.6 kcal/mol) is less than that leading to the seven (18.4 kcal/mol) and suggest that it ought to be the faster process. While AM1 calculations are convenient because they require so little time to complete, the results are often not very accurate. Consequently, we repeated the calculations using density functional theory (UB3LYP/6-31G(d)). In *each* instance the migrations are predicted to occur via a nearly barrierless process (viz., <1 kcal/mol), [1a] whose magnitudes differ by roughly 0.5 kcal/mol. The values are clearly too close to claim that the potential differences are or are not of a kinetic origin.

Another possibility is that the oxidation of **5** is centered on the ketal rather than the housane framework and that the ketal is easier to oxidize. The voltammogram for the ethylene glycol ketal of cyclohexanone displayed an E_p value of +2.4 V (vs $Ag/AgNO_3$), thus clearly dispelling the notion. Consistent with the idea that the oxidation is housane centered is the HOMO surface map, resulting from a B3LYP/6-31G(d) calculation, and pictured in Figure 3.

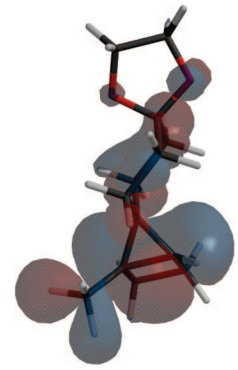

FIGURE 3. HOMO surface for the daucene precursor.

Given these findings, we elected to modify our analysis so that it focused upon determining why the housanes that bear electronegative substituents are more difficult to oxidize than those that do not. Table 1 summarizes the B3LYP/6-31G(d)-calculated HOMO energies for five housanes. The HOMO

(10) Wu, X.; Davis, A. P.; Fry, A. J. *Org. Lett.* **2007**, *9*, 5633–5636.

(11) (a) That the second wave in each voltammogram corresponds to the products was confirmed by overlaying the curves of products with the curves shown in Figure 2. (b) Notice the broad, ill-defined nature of the voltammograms, independent of whether the benzyloxy groups was present or absent.

(12) Consideration of the Nernst equation reveals how this is so. Thus, the faster the rate of the process that follows the initial redox equilibrium, the larger will be the factor that is subtracted. The consequence, of course, is to make easier the redox process being studied. For a beautiful example of these thoughts and their consequences, refer to: Moeller, K. D.; Tinao, L. V. *J. Am. Chem. Soc.* **1992**, *114*, 1033–1041.

TABLE 1. Calculated HOMO Energies for Five Housanes

	E(HOMO) eV; B3LYP/6-31G(d)		E(HOMO) eV; B3LYP/6-31G(d)
 **21**	–6.59 [not oxidizable by $(p\text{-}BrC_6H_4)_3N^{\ddagger}$]	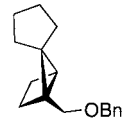 **1**	–6.48 (oxidizable)
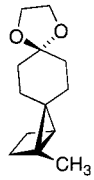 **5**	–6.43 (oxidizable)	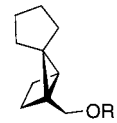 **18 a, b**	**18 a**, R = CH_3, see text **18 b**, R = H, –6.61 eV at +154° and –6.44 at –71°

energies serve as a guide to oxidizability, viz. the more negative the value, the more difficult the substance ought to be to oxidize.

A cursory examination of the data reveals an interesting point, viz., the HOMO energy for the hydroxymethyl-substituted housane **18b** appears to vary as a function of the dihedral angle between the cyclopropyl unit and the C−O bond. Notice also that the methyl-substituted housane **5** is predicted to be easier to oxidize than either **18a** or **18b**, both of which have an electron-withdrawing group. Though in a context that differs from ours, Fry and Yoshida have independently observed very significant stereoelectronic effects upon redox potentials.[13]

We suspected that there might be a stereoelectronic component to the HOMO energy for systems that bear an electronegative group appended to a bridgehead carbon. The magnitude of the effect ought to vary as a function of the ability of the substituent to interact with the bent bonds exemplified by the Walsh orbitals of the cyclopropyl subunit. To explore this notion, we carried out B3LYP/6-31G(d) calculations on **18a**. The results, portrayed in Figure 4, are revealing. Shown there is a plot illustrating the way in which the HOMO energy, as well as the relative energy for each of 15 conformers, varies as a function of the dihedral angle between the cyclopropyl and C−O subunits, C1,C4,C10,O1. Shown too is the Boltzmann distribution over the range of angles −180 to +180°.

Notice that the HOMO energies range from a high of −6.31 eV at −125°, to −6.47 eV when the dihedral angle is −75°, and reaches a low of −6.62 eV for the most highly populated conformer (+150°). Two conformers are dominant, one at a dihedral angle of −75° and the other at +150°.

What is the origin of these effects? Why, for example, should the conformer whose dihedral angle is −75° be of lower energy than others? And why should its HOMO energy be deeper than that for the methyl substituted framework exemplified by the daucene precursor **5**?

To address these questions, we looked for and were able to identify interactions between the cyclopropyl and C−O units in the surface corresponding to the HOMO at this dihedral angle. Shown on the left of Figure 5 is a slice of the HOMO surface near the cyclopropyl framework that is clearly Walsh-like. Shown in the middle is a slice that is coincident with the C−O bond; it resembles lone pair orbitals on oxygen. The slices suggest the existence of a through-space interaction between the orbitals on oxygen and the Walsh subunits. This is confirmed by examining the representation shown on the right; it reveals the entire HOMO surface. Despite its complex appearance, the through space interaction is clearly evident; so too is a stabilizing interaction between the Walsh framework and one of the C−H bonds of the connecting CH_2 unit. Together, these interactions ought to stabilize the molecule and also deepen the energy of the HOMO.

When the dihedral angle corresponds to that of the dominant conformation (viz. to +150°), the HOMO surface is also complex (Figure 6). Though it is difficult to assess with confidence the existence of interactions other than that between the Walsh orbital and one of the C−H bonds of the intervening CH_2 unit, use of Weinhold's natural bond orbital (NBO) method suggests the possibility of a lone pair Walsh orbital interaction as well.[14]

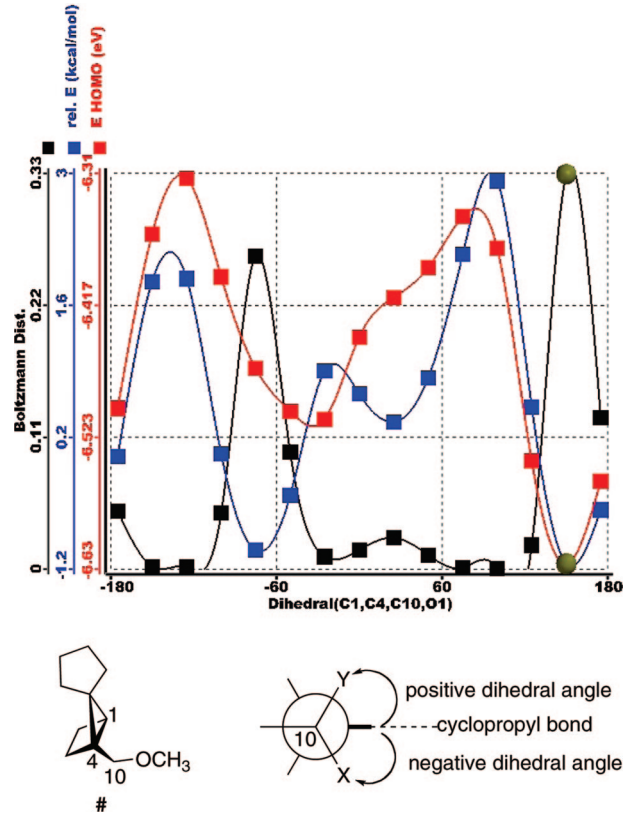

FIGURE 4. Energy profile for housane **18a** as a function of the dihedral angle (C1, C4, C10, O1). The numbering 1, 4, 10 is a consequence of the numbering system used in the quantum calculations.

(13) (a) Kaimakliotis, C.; Fry, A. J. *J. Org. Chem.* **2003**, *68*, 9893–9898. (b) Yoshida, J-I.; Maekawa, T.; Murata, T.; Matsunaga, S-i.; Ism, S. *J. Am. Chem. Soc.* **1990**, *112*, 1962–1970.

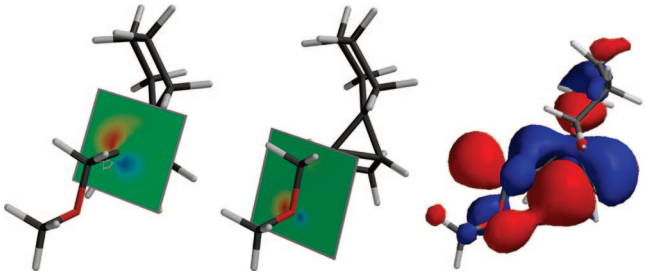

FIGURE 5. Slices through the HOMO surface near the cyclopropane and through the C−O bond. The HOMO surface is shown on the right.

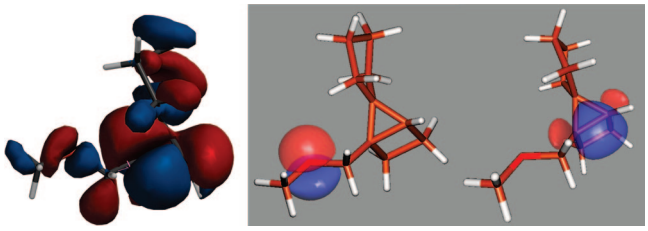

FIGURE 6. The HOMO surface for the lowest energy conformer is shown on the left. The natural bond orbitals (NBO's) are illustrated in the middle and on the right.

Together, the dominant conformers account for 59% of the total distribution. Given the fact that the energy of the HOMO depends upon the dihedral angle and that the remaining 41% of the conformer distribution will also be populated during the time frame of the CV experiment, *we suggest that broadness of the curve for the ROCH$_2$-substituted systems is the result of a time-averaged sampling of the HOMO energies over the distribution of conformers*.[15]

Concluding Remarks

Through the investigations described herein, we have gained additional understanding of the properties of housane cation radicals and of the factors that regulate the regioselectivity of their rearrangements. We have demonstrated that the chemistry can be applied to the synthesis of a natural product and look forward to using it to assemble more complex systems. Is the preceding mechanistic discussion generalizable to other systems? Will it be useful? Can it be used, for example, to allow one to selectively oxidize one vs another functional unit when the two differ in the manner in which they interact with an electrophore? We intend to examine these opportunities.

Experimental Section

Cyclic Voltammetry. Cyclic voltammograms were recorded in a single cell, constructed from a glass vial, fitted with three electrodes. A glassy carbon disk electrode (0.033 cm^2 surface area) was used as a working electrode and a platinum wire (0.6 cm^2 surface area) was used as a counter electrode. The potential was recorded with the reference electrode Ag/0.01 M $AgNO_3$ immersed in 0.1 M solution of *n*-Bu_4NBF_4 in CH_3CN that was separated from the medium by a Vycor membrane. Its potential is +0.35 V versus the aqueous saturated calomel electrode (SCE). All solutions were deoxygenated with a stream of argon for 20 min before each experiment. A scan rate of 200 mV/s was used. Cyclic voltammetry (CV) was performed using a computer-controlled potentiostat, and data were collected using the software available from Cypress (version 1.5.5) and exported to an Excel Microsoft worksheet.

General Procedure for Preparative Indirect Electrolysis. All preparative electrolyses were carried out in an undivided cell fitted with a platinum anode (1 cm^2 surface area) as a working electrode and a reticulated vitreous carbon (RVC) electrode as a counter electrode. The Ag/0.01 M $AgNO_3$ reference electrode used for the electrolyses has a potential of +0.35 V versus the saturated aqueous calomel electrode (SCE) at 25 °C. Therefore, the conversion of the potentials recorded herein to values referenced to SCE requires the subtraction of 0.35 V. The separation between the each of the electrodes was ca. 0.5 cm. The potentials of all reactions were controlled by a potentiostat, and the amount of charge passed was monitored using a coulometer.

In a preparative cell, constructed from a simple glass vial, a 0.1 M solution of *n*-Bu_4NBF_4 in CH_3CN was added. All electrodes were inserted through predrilled holes in a piece of Teflon that was positioned at the top of the cell. The solution was then deoxygenated by bubbling argon through it for 20 min. A pre-electrolysis was conducted at constant potential of 880 mV until the current value dropped to ca. 0.5 mA. We routinely carry out pre-electrolyses in order to ensure the absence of any redox active materials at the time when the substrate is added to the reaction

Housane and 10−40 mol % of tris(4-bromophenyl)amine were added to the solution. When a potential of +880 mV was applied to the cell, the current flow increased, and a blue-green color appeared on the surface of platinum electrode indicating the oxidation of the mediator and the presence of the aminium cation radical. The course of the reaction was monitored by TLC or GCMS; the electrolysis was stopped after the coulometer indicated that at least more than 1 F/mol of charge had passed, the exact amount depending upon the degree of consumption of the starting material. At the end of a run, the dark yellow solution was concentrated under reduced pressure, the resulting material was washed with water, and then extracted with Et_2O. The combined organic portions were washed with brine, dried over Na_2SO_4, and concentrated under reduced pressure at room temperature. The products were purified by flash chromatograph on Si_2O using the conditions specified.

Alkylation of 11: Preparation of 1-Methyl-9,12-dioxadispiro-[4.2.4.2]tetradec-3-en-2-one. To a solution of diisopropylamine (1.01 mL, 8.85 mmol) in dry THF (20 mL) at 0 °C was added *n*-BuLi (2.2 M in hexanes, 3.5 mL, 7.7 mmol). After being stirred for 40 min, the solution was cooled to −78 °C and a solution of the cyclopentenone **11** (800 mg, 3.85 mmol) in THF (15 mL) was added dropwise. The solution was stirred for 1 h, and the cooling bath was removed. While the temperature of reaction solution was warming gradually, iodomethane (0.32 mL, 5.01 mmol) in THF (2 mL) was added dropwise. After further stirring for 2 h, the reaction was quenched with saturated aqueous NH_4Cl (25 mL) and the organic layer was separated. The aqueous layer was extracted with ether (5 × 30 mL). The combined organic portions were washed with brine (30 mL), dried over anhydrous Na_2SO_4, filtered, and concentrated under reduced pressure. The crude product was purified by flash chromatography on silica gel (petroleum ether/Et_2O 4:6, R_f = 0.28, vanillin) to afford the monoalkylated product as a white powder (386 mg, 1.74 mmol, 45%). A dimethylated compound (129 mg, 0.546 mmol) was also obtained, and the starting cyclopentenone (301 mg, 1.48 mmol) was recovered: IR (neat) ν_{max} 3060, 2938, 2881, 1710, 1587, 1448, 1338, 1105, 947, 879, 823 cm^{-1}; ^{1}H NMR (400 MHz, $CDCl_3$) δ 1.06−1.13 (d, J = 7.52 Hz, 3H), 1.36−1.45 (m, 1H), 1.56−1.67 (m, 2H), 1.69−1.76 (m, 3H), 1.79−1.86 (m, 2H), 2.08−2.16 (q, J = 7.52 Hz, 1H), 3.95 (s, 4H), 6.11 (d, J = 5.84 Hz, 1H), 7.81 (d, J = 5.84 Hz, 1H); ^{13}C NMR (100 MHz, $CDCl_3$) δ 11.1, 30.7, 31.8, 32.1, 34.9, 47.1, 51.5, 64.5, 108.1, 131.6, 168.9, 211.8; LRMS (ESI+/TOF) *m/z* 223 [M + H]$^+$, 245 [M + Na]$^+$, 467 [2 M + Na]$^+$; HRMS (ESI+/TOF) found 245.1151, calcd for 245.1148 for $C_{13}H_{18}O_3Na$.

(14) Foster, J. P.; Weinhold, F. *J. Am. Chem. Soc.* **1980**, *102*, 7211–7218.
(15) The broad, ill-defined nature of the voltammograms is reminiscent of the lack of definition that is often encountered in ultraviolet absorption spectra.

Luche Reduction of 11: Formation of 1-Methyl-9,12-dioxadispiro[4.2.4.2]tetradec-3-en-2-ol. The methylated cyclopentenone (500 mg, 2.25 mmol) and $CeCl_3 \cdot 7H_2O$ (838 mg, 2.25 mmol) were dissolved in methanol (8 mL). $NaBH_4$ (105 mg, 2.70 mmol) was added in one portion with stirring; vigorous gas evolution occurred. The reaction mixture was stirred for 20 min and then quenched using H_2O (5 mL). The organic layer was separated, and the aqueous layer was extracted with ether (5 × 10 mL). The combined organic portions were washed with brine (15 mL), dried over anhydrous Na_2SO_4, filtered, and concentrated under reduced pressure. The crude product was chromatographed on silica gel (petroleum ether/Et_2O 3:7, R_f = 0.25, vanillin) to afford the diastereomeric mixture of the cyclopentenols as a colorless liquid (367 mg, 1.64 mmol, 73%). The diastereomeric mixture was subjected to the dehydration after confirming its presence by IR and GCMS (HP 5890A gas chromatography with ZB-5MS column (30 m × 0.25 mm × 0.25 df (μm), 5% polysilarylene dimethylpolysiloxane) and HP 5970 mass selective detector (EI), initial temperature 50 °C, initial time 2 min, ramp 20 °C/min, final temperature 300 °C, final time 10 min). The GCMS and ^{1}H NMR data indicated the diastereomers to be produced in the ratio of 1:1; they were not separated since both the methyl and OH bearing carbons are to be converted to sp^2-hybridized centers: IR (neat) ν_{max} 3435, 3047, 2947, 2881, 1448, 1373, 1290, 1176, 1103, 1036,947, 881 cm^{-1}; LRMS (EI) one diastereomer 224 (1), 206 (2), 144 (1), 119 (1), 99 (100), 86 (26), the other diastereomer 224 (1), 206 (1), 169 (1), 144 (1), 125 (1), 99 (100), 86 (23).

Preparation of 1-Methyl-9,12-dioxadispiro[4.2.4.2]tetradec-1,3-diene (12). To a solution of the alcohol (302 mg, 1.35 mmol) and Et_3N (0.66 mL, 4.72 mmol) in benzene (13 mL) was added methanesulfonic anhydride (606 mg, 3.38 mmol). The resulting mixture was stirred at rt for 3 h before water (10 mL) was added, and the aqueous layer was extracted with Et_2O (5 × 20 mL). The combined organic layers were washed with brine (30 mL), dried over anhydrous Na_2SO_4, filtered, and concentrated under reduced pressure. This material was purified by flash chromatography (SiO_2, petroleum ether/Et_2O 9:1, R_f = 0.38, UV, vanillin) to give the cyclopentadiene **12** (247 mg, 1.20 mmol, 89%) as a colorless oil: IR (neat) ν_{max} 3064, 2931, 2881, 1608, 1536, 1442, 1365, 1105, 951, 881, 728 cm^{-1}; ^{1}H NMR (400 MHz, $CDCl_3$) δ 1.01 − 1.07 (m, 2H), 1.82 − 1.84 (m, 3H), 1.84 −1.95 (m, 6H), 3.98 (s, 4H), 5.91 (m, 1H), 6.32 (dd, J = 1.84, 5.68 Hz, 1H), 6.67 (dd, J = 1.23, 5.68 Hz, 1H); ^{13}C NMR (100 MHz, $CDCl_3$) δ 12.7, 29.6, 34.2, 56.1, 64.5, 64.6, 108.9, 124.1, 130.1, 139.7, 153.9; LRMS (EI) 206 (29), 178 (5), 161 (9), 144 (81), 129 (52), 105 (95), 99 (100), 92 (93), 77 (20); HRMS (EI) found 206.1305, calcd 206.1307 for $C_{13}H_{18}O_2$.

Preparation of Bis(2,2,2-trichloroethyl) 4′,4′-Ethylenedioxy-1-methyl-2,3-diazaspiro[bicyclo[2.2.1]heptane-7,1′-cyclohexane]-2,3-dicarboxylate (13). The spirocyclohexyl cyclopentadiene derivative **12** (247 mg, 1.20 mmol) and bis(2,2,2-trichloroethyl) azodicarboxylate (538 mg, 1.32 mmol) were dissolved in dry CH_2Cl_2 (13 mL), and the resulting mixture was stirred for 12 h. The resulting yellow solution was concentrated under reduced pressure after TLC analysis (vanillin) showed that the starting cyclopentadiene **12** was consumed. The solution of the cycloadduct in EtOAc (15 mL) was charged with 10% Pd−C catalyst (127 mg) and stirred vigorously under hydrogen gas at atmospheric pressure for 12 h. The catalyst was filtered through a pad of Celite, and the filtrate was concentrated under reduced pressure. The resulting hydrogenation product was purified by flash chromatography on silica gel (petroleum ether/Et_2O 5:5, R_f = 0.30, vanillin) to provide the biscarbamate **13** as white foam (650 mg, 1.10 mmol, 92% over two steps): IR (neat) ν_{max} 2954, 2884, 1718, 1450, 1382, 1319, 1280, 1224, 1109, 1059, 800, 719 cm^{-1}; ^{1}H NMR (400 MHz, $CDCl_3$) δ 1.24 − 1.35 (m, 1H), 1.40 − 1.51 (m, 2H), 1.54 − 1.59 (m, 3H), 1.59 − 1.68 (m, 4H), 1.69 − 1.88 (m, 4H), 1.92 − 2.09 (m, 2H), 3.89 − 4.03 (s, 4H), 4.59 − 5.10 (m, 4H); LRMS (ESI+/TOF) m/z 608 [M + Na]$^+$; HRMS (ESI+/TOF) found 608.9655, calcd 608.9657 for $C_{19}H_{24}N_2O_6NaCl_6$. Note that the poorly resolved proton NMR spectrum for the biscarbamate is typical. This class of compounds undergoes several dynamic phenomena under the ambient conditions of an NMR experiment. Thus, we chose to assess purity after the next step in the reaction sequence.

Preparation of Diazene 14: 4′,4′-Ethylenedioxy-1-methyl-2,3-diazaspiro[bicyclo[2.2.1]hept[2]ene-7,1′-cyclohexane]. The biscarbamate **13** (630 mg, 1.07 mmol) was dissolved in EtOH (8 mL), and KOH (1.2 g, 21.4 mmol) was added. The resulting mixture was brought to reflux for 12 h. The reaction mixture was cooled to room temperature and diluted with EtOH (4 mL). Following removal of the reflux condenser and cooling to 0 °C, a solution of $K_3Fe(CN)_6$ (3.52 g, 10.69 mmol) in water (10 mL) was added slowly using a dropping funnel over a period of 30 min, and the mixture was stirred for 12 h at room temperature. A Cu(I) test for the resulting diazene was positive. After the mixture was diluted with water (10 mL), the product was extracted with Et_2O (5 × 30 mL), washed with brine (30 mL), and dried over anhydrous $MgSO_4$. The crude product was obtained upon concentration under reduced pressure. Purification by flash chromatography on silica gel (petroleum ether/Et_2O 5:5, R_f = 0.15, Cu(I) stain, vanillin) to afford the diazene **14** as a yellow solid (203 mg, 0.860 mmol, 80%): IR (neat) ν_{max} 2958, 2883, 1471, 1442, 1380, 1157, 1105, 1033, 947 cm^{-1}; ^{1}H NMR (400 MHz, $CDCl_3$) δ 0.80−0.9 (m, 1H), 0.93−1.08 (m, 2H), 1.13−1.24 (m, 1H), 1.27−1.34 (m, 1H), 1.40−1.49 (m, 2H), 1.49−1.61 (m, 6H), 1.61−1.73 (m, 2H), 3.83−3.95 (m, 4H), 4.98−5.09 (d, J = 2.61 Hz, 1H); ^{13}C NMR (100 MHz, $CDCl_3$) δ 12.2, 19.8, 23.1, 25.6, 26.1, 32.8, 32.9, 56.5, 64.4, 64.5, 108.3; LRMS (CI/CH_4) m/z 237 (74), 209 (100), 193 (22), 179 (11), 165 (19), 146 (13), 99 (45); HRMS (CI/CH_4) found 237.1598, calcd 237.1603 for $[C_{13}H_{20}N_2O_2 + H]^+$.

Preparation of Housane 5: 4′,4′-Ethylenedioxy-1-methylspiro-[bicyclo[2.1.0]pentane-5,1′-cyclohexane]. The diazene **14** (160 mg, 0.678 mmol) was weighed into a 25 mL Pyrex round-bottomed flask and dissolved in dry THF (5 mL). The solution was degassed by bubbling argon through it for 20 min. Then, the solution was irradiated with UV light of 365 nm from a UV hand lamp placed adjacent to the flask; the course of the reaction was followed by TLC (vanillin). After 16 h, the diazene was consumed, and the solvent was evaporated under reduced pressure at room temperature. The crude product was chromatographed on silica gel (petroleum ether/Et_2O 9:1, R_f = 0.38, vanillin) to afford the housane **5** as a colorless liquid (126 mg, 0.601 mmol, 89%): IR (neat) ν_{max} 2943, 2866, 1446, 1365, 1242, 1147, 1119, 1093, 1038, 947, 916 cm^{-1}; ^{1}H NMR (400 MHz, $CDCl_3$) δ 1.09−1.15 (dd, J = 1.54, 4.61 Hz, 1H), 1.2−1.23 (s, 3H), 1.23−1.28 (m, 2H), 1.43−1.51 (m, 1H), 1.53−1.60 (m, 2H), 1.65−1.70 (m, 5H), 1.75−1.84 (m, 1H), 1.93−2.03 (m, 1H), 3.36−4.01 (m, 4H); ^{13}C NMR (100 MHz, $CDCl_3$) δ 16.0, 17.5, 20.4, 26.1, 27.8, 28.2, 29.2, 30.2, 34.4, 34.5, 64.4, 110.0; LRMS (EI) 208(5), 193 (4), 179 (9), 163 (6), 146 (6), 131 (10), 107 (2), 99 (100), 93 (33), 83 (70), 79 (42); HRMS (EI) found 208.1456, calcd 208.1463 for $C_{13}H_{20}O_2$.

Formation of the [5.3.0] Adduct, 8a-Methyl-2,4,5,7,8,8a-hexahydro-1*H*-spiro[azulene-6,2′-[1,3]dioxolane] (7). In a preparative cell fitted with a platinum anode (1 cm^2 surface area) as the working electrode, a reticulated vitreous carbon (RVC) electrode as the counter electrode and a Ag/0.01 M $AgNO_3$ reference electrode, a 0.1 M solution of n-Bu_4NBF_4 in CH_3CN (10 mL) was added. The solution was deoxygenated by bubbling argon through it for 20 min. A pre-electrolysis was conducted at a controlled potential of 880 mV until the current value dropped to ca. 0.5 mA. Housane **5** (20 mg, 0.096 mmol) and 20 mol % of tris(4-bromophenyl)amine (10 mg, 0.020 mmol) were added to the solution. When a potential of +880 mV was applied to the cell, current flow occurred. The reaction was monitored by GCMS using a 30 m × 0.25 mm × 0.25 μm, 5% polysilarylene dimethylpolysiloxane capillary column and mass selective detector (EI; initial temperature 50 °C, initial time 2 min, ramp 20 °C/min, final temperature 300 °C, final time 10 min). While the reaction was being monitored by GCMS, the

electrolysis was stopped by turning the potentiostat off. After 50 min, GCMS analysis showed that the starting housane still remained; the current continued to drop. Another 20 mol % of tris(4-bromophenyl)amine was added in order to consume the housane, and the electrolysis was stopped when GCMS analysis indicated that the starting was completely consumed (after an additional 30 min). The resulting solution was concentrated under reduced pressure, filtered through a silica plug, and flushed with diethyl ether. The filtrate was concentrated again under reduced pressure at room temperature. The crude product was purified by flash chromatography on Si_2O (petroleum ether/Et_2O 9.5:0.5, $R_f = 0.24$, vanillin) to afford the bicyclodecene adduct **7** as a colorless liquid (14 mg, 0.067 mmol, 70%): IR (neat) ν_{max} 3035, 2941, 2879, 2860, 1450, 1367, 1265, 1103, 1045, 993, 926, 875, 821 cm^{-1}; ^1H NMR (400 MHz, $CDCl_3$) δ 0.92−0.98 (s, 3H), 1.43−1.51 (m, 2H), 1.58−1.74 (m, 5H), 1.87−1.98 (m, 2H), 2.07−2.15 (m, 1H), 2.21−2.33 (m, 2H), 3.85−3.96 (m, 4H), 5.26−5.38 (s, 1H); ^{13}C NMR (100 MHz, $CDCl_3$) δ 22.7, 25.4, 29.2, 33.0, 33.3, 39.1, 40.8, 48.9, 64.3, 64.5, 112.1, 124.1, 152.7; LRMS (EI) 208 (18), 193 (5), 179 (14), 163 (5), 149 (7), 122 (8), 107 (10), 99 (100), 93 (18), 79 (21); HRMS (EI) found 208.1471, calcd 208.1463 for $C_{13}H_{20}O_2$.

Chemical Electron Transfer Method. To the stirred solution of the housane **5** (20 mg, 0.096 mmol) and 2,6-di-*tert*-butylpyridine (11 μL, 0.048 mmol) in dry methylene chloride (1 mL) was added tris(4-bromophenyl)aminium hexachloroantimonate (16 mg, 0.16 mmol). After approximately 5 min, the blue solution changed into a dark yellow color. Another 20 mol % of tris(4-bromophenyl)aminium hexachloroantimonate was added to maintain the blue color; the solution was allowed to stir for another 25 min. The reaction mixture was then passed through a short column of oven-dried basic alumina and concentrated in vacuo. The crude was chromatographed on silica gel (petroleum ether/Et_2O 9.5:0.5, R_f = 0.24, vanillin) to afford the bicyclodecene **7** as a colorless liquid (17 mg, 0.082 mmol, 85%). Spectral data is shown in the previous section of indirect electrolysis.

Preparation of 1-Isopropyl-3a-methyl-3,3a,4,5,7,8-hexahydroazulen-6(2*H*)-one (16). Into a round-bottomed flask are added lithium borohydride (13 mg, 0.557 mmol) in THF (6 mL) and the alkene **7** (232 mg, 1.11 mmol). The flask was immersed in a water bath at 25 °C. Boron trifluoride etherate (154 μL, 1.22 mmol) was added slowly. After being stirred for 5 h, the solution was treated with water (3−4 drops), followed by 3 M NaOH (0.57 mL, 1.70 mmol) and 30% H_2O_2 (0.34 mL, 3.34 mmol). The resulting solution was allowed to stir for 2 h, and then the mixture was concentrated under reduced pressure. The residue was dissolved in ether (5 mL) and H_2O (3 mL). The aqueous layer was extracted with ether (5 × 5 mL), and the combined extracts were washed with brine (5 mL), dried over anhydrous Na_2SO_4, and concentrated under reduced pressure. A solution of the crude carbinol in CH_2Cl_2 (8 mL) at 0 °C was treated with PDC (712 g, 1.89 mmol) and 4 Å molecular sieves (700 mg). The mixture was allowed to stir at 0 °C for 0.5 h and then warmed to room temperature and stirred for 8 h. The mixture was diluted with ether (5 mL), treated with Celite (600 mg), and filtered through a pad of Celite. The filtrate was concentrated under reduced pressure and was chromatographed on silica gel (petroleum ether/Et_2O 5:5, $R_f = 0.31$, vanillin) to afford the expected ketone as a colorless liquid (139 mg, 0.62 mmol, 56%): IR (neat) ν_{max} 2929, 2870, 1737, 1589, 1465, 1373, 1165, 1124, 910 cm^{-1}; ^1H NMR (400 MHz, $CDCl_3$) δ 1.11−1.15 (s, 3H), 1.51−1.58 (m, 3H), 1.63−1.67 (m, 2H), 1.71−1.81 (m, 5H), 1.84−1.90 (m, 1H), 2.18−2.43 (m, 2H), 3.76−4.05 (s, 4H); ^{13}C NMR (100 MHz, $CDCl_3$) δ 22.2, 28.1, 29.9, 33.1, 33.5, 36.3, 36.7, 38.2, 60.2, 64.4, 64.5, 111.5, 222.7; LRMS (EI) 224 (4), 195 (3), 167 (2), 149 (10), 139 (3), 99 (100), 86 (18); HRMS (EI) found 224.1420, calcd 224.1412 for $C_{13}H_{20}O_3$.

The ketone was converted to a mixture of three inseparable isomeric alkenes that were equilibrated using perchloric acid to form structure **16**, the thermodynamically most stable form. The sequence began with the addition of the isopropyl substructure. Thus, anhydrous cerium chloride was obtained by heating $CeCl_3 \cdot 7H_2O$ at 100 °C in vacuum for 12 h using an Abderhalden drying apparatus. Anhydrous cerium chloride (308 mg, 1.25 mmol) and the ketone (140 mg, 0.625 mmol) were dissolved in THF (3 mL) and stirred for 2 h at rt. Isopropyllithium (0.7 M in hexane, 2.7 mL, 1.88 mmol) was added dropwise with stirring, resulting in a light purple suspension. After being stirred for 12 h, the reaction was quenched with saturated NH_4Cl (4 mL) and the aqueous layer was extracted with Et_2O (5 × 5 mL). The combined organic layers were washed with brine (5 mL), dried over Na_2SO_4, filtered, and concentrated under reduced pressure to afford the diastereomeric mixture of the desired alcohol and the starting ketone, as a yellow oil. The crude material was subjected to next dehydration step without purification. An infrared spectrum verified the presence of the hydroxyl group: IR (neat) ν_{max} 3513, 2951, 2877, 1452, 1371, 1103, 1035, 945 cm^{-1}.

To a solution of the crude mixture of the alcohol diastereomers (0.625 mmol) and the starting ketone and Et_3N (0.39 mL, 2.19 mmol) in benzene (4 mL) was added methanesulfonic anhydride (393 mg, 2.19 mmol). The resulting mixture was stirred at rt for 6 h before saturated NH_4Cl (3 mL) was added, and the aqueous layer was extracted with Et_2O (5 × 5 mL). The combined organic layers were washed with brine (5 mL), dried over anhydrous Na_2SO_4, filtered, and concentrated under reduced pressure. This crude material was purified by flash chromatography (hexanes/EtO_2 9:1, $R_f = 0.36$, vanillin) to give the mixture of three alkene isomers (69 mg, 0.275 mmol, 43%) as a yellow oil. The ketone (48 mg, 0.213 mmol) was recovered and could be reused. GCMS analysis using a 30 m × 0.25 mm × 0.25 μm, 5% polysilarylene dimethylpolysiloxane capillary column and mass selective detector (EI; initial temperature 50 °C, initial time 2 min, ramp 20 °C/min, final temperature 300 °C, final time 10 min) showed a ratio of 13:53:34 for the isomeric alkenes.

Isomerization of the inseparable mixture was accomplished as follows. The alkenes (20 mg, 0.080 mmol) and 70% $HClO_4$ (55 μL, 0.64 mmol, 8 equiv) were dissolved in $CHCl_3$ (2 mL) and stirred for 30 min. The resulting yellow solution was neutralized with saturated $NaHCO_3$ (1 mL), and the aqueous layer was extracted with EtO_2 (5 × 2 mL). The combined organic layers were washed with brine (2 mL), filtered through a silica plug, and concentrated under reduced pressure. The crude product was chromatographed on 10% silver ion impregnated silica gel[16] (pentane/Et_2O 9:1, R_f = 0.22, vanillin) to afford the isomerized deprotected keto alkene **16** as a colorless liquid (8 mg, 0.039 mmol, 48%): IR (neat) ν_{max} 2956, 2850, 1702, 1460, 874, 856 cm^{-1}; ^1H NMR (400 MHz, $CDCl_3$) δ 0.92−0.97 (d, J = 6.91 Hz, 3H), 0.97−1.00 (d, J = 6.91 Hz, 3H), 1.01−1.05 (s, 3H), 1.57−1.67 (m, 4H), 1.99−2.09 (m, 1H), 2.18−2.26 (m, 2H), 2.27−2.40 (m, 2H), 2.46−2.59 (m, 3H), 2.59−2.69 (septet, J = 6.91 Hz, 1H); ^{13}C NMR (100 MHz, $CDCl_3$) δ 19.8, 21.6, 22.2, 24.5, 27.5, 28.0, 36.5, 38.2, 40.0, 43.8, 50.3, 138.4, 143.3, 215.0; LRMS (EI) 206 (33), 191 (33), 173 (3), 163 (100), 149 (26), 135 (50), 121 (66), 107 (31), 91 (42), 84 (37), 77 (27); HRMS (EI) found 206.1677, calcd 206.1671 for $C_{14}H_{22}O$.

Preparation of 3-Isopropyl-6,8a-dimethyl-1,2,4,5,8,8a-hexahydroazulene (Daucene, 6). Anhydrous cerium chloride (27 mg, 0.109 mmol) and the ketone **16** (15 mg, 0.0728 mmol) were dissolved in THF (2 mL) and stirred for 2 h at rt. The methylmagnesium bromide (3 M in diethyl ether, 0.10 mL, 0.291 mmol) was added dropwise with stirring. After being stirred for 12 h, the reaction mixture was quenched with saturated NH_4Cl (1 mL), and the aqueous layer was

(16) (a) Pigulevkii, G. V.; Kivaleva, V. I. *Doklady Akad. Nauk S.S.S.R.* **1961**, *141*, 1382. (b) Sriraman, M. C.; Nagasampagi, B. A.; Pandey, R. C.; Dev, S. *Tetrahedron* **1973**, *29*, 985–991. (c) Audenaert, F.; Keukeleire, D. D.; Vandewalle, M. *Tetrahedron* **1987**, *43*, 5593–5604. (d) Naegeli, P.; Kaiser, R. *Tetrahedron Lett.* **1972**, *13*, 2013–2016. (e) Seto, H.; Fujimoto, Y.; Tatsuno, T.; Yoshioka, H. *Synth. Commun.* **1985**, *15*, 1217–1224. (f) Mehta, G.; Krishnamurthy, N. *Synth. Commun.* **1985**, *18*, 1267–1274. (g) Momchilova, S.; Nikolova-Damyanova, B. J. *Sep. Sci.* **2003**, *26*, 261–270.

extracted with Et_2O (5 × 2 mL). The combined organic layers were washed with brine (2 mL), dried over Na_2SO_4, filtered, and concentrated under reduced pressure to afford a mixture of diastereomeric alcohols and the starting ketone as a white oil. The crude mixture was subjected to next dehydration step without purification: IR (neat) ν_{max} 3430 (OH), 2956, 2890, 1702, 1457, 1371, 1108 cm^{-1}. To a solution of the crude mixture of alcohol diastereomers (0.0728 mmol) and unreacted ketone **16**, and Et_3N (61 μL, 0.437 mmol) in benzene (2 mL) was added methanesulfonic anhydride (38 mg, 0.218 mmol). The resulting mixture was stirred at rt for 6 h. Saturated NH_4Cl (1 mL) was added, and the aqueous layer was extracted with Et_2O (5 × 2 mL). The combined organic layers were washed with brine (2 mL), dried over anhydrous Na_2SO_4, filtered, and concentrated under reduced pressure. Purification by flash chromatography (10% $AgNO_3$−silica gel, pentane/EtO_2 9.7:0.3, R_f = 0.62 by silica gel coated TLC, vanillin) gave daucene (**6**; 4 mg, 0.020 mmol, 27%,) as an oil, along with the isomeric endocyclic alkene wherein elimination occurred in the alternative direction (3 mg, 0.015 mL, 21%, R_f = 0.62). The starting ketone **16** (4 mg, 0.019 mmol, 26%) was also recovered. The spectral data was in accordance that reported in the literature: IR (neat) ν_{max} 2956, 2927, 2862, 1639, 1454, 1367, 1203, 1105, 887, 827 cm^{-1}; ^1H NMR (400 MHz, $CDCl_3$) δ 0.91 (s, 3H), 0.93 (d, J = 6.75 Hz, 3H), 0.98 (d, J = 6.75 Hz, 3H), 1.48 − 1.65 (m, 3H), 1.74 (s, 3H), 1.81 (m, 1H), 1.90 − 2.05 (m, 3H), 2.12 − 2.21 (m, 2H), 2.39 (m, 1H), 2.66 (septet, J = 6.75 Hz, 1H), 5.42 (m, 1H); ^{13}C NMR (100 MHz, $CDCl_3$) δ 21.4 (primary), 22.1 (primary), 22.7 (secondary), 23.7 (primary), 26.2 (tertiary), 26.6 (primary), 27.3 (secondary), 33.7 (secondary), 38.7 (secondary), 40.6 (secondary), 49.7 (quaternary), 122.9 (tertiary), 138.9 (quaternary), 140.0 (quaternary), 142.1 (quaternary); LRMS (EI) 204, 189, 161, 136, 121, 106, 91, 79, 67; HRMS (EI) found 204.1875, calcd 204.1878 for $C_{15}H_{24}$.

Quantum Calculations. Calculations were carried out using either Spartan ′04 for Macintosh or Spartan ′08 for PC.[9]

Acknowledgment. R.D.L. is grateful to Dr. Kalju Kahn (UCSB) for carrying out the NBO analysis, to Professor Bernie Kirtman (UCSB) for interesting discussions, to Professor Dean Tantillo (UC Davis) for the suggestion to examine the NBO approach, and to Dr. James Gerken (Caltech) for enlightening correspondence. We express our sincere gratitude to Amgen and the Petroleum Research Fund, administered by the American Chemical Society (ACS PRF no. 43443-AC1), each for partial support of this research.

Supporting Information Available: NMR data for compounds **11** (^1H), **12** (^1H and ^{13}C), **13** (^1H), **14** (^1H and ^{13}C), **5** (^1H and ^{13}C), **7** (^1H and ^{13}C), **16** (^1H and ^{13}C), and **6** (^1H and ^{13}C). This material is available free of charge via the Internet at http://pubs.acs.org.

JO801199S